THE ROYAL SOCIETY

Received 15 April 2002
Accepted 16 September 2002
Published online 12 December 2002

Top-down or bottom-up regulation of intra-host blood-stage malaria: do malaria parasites most resemble the dynamics of prey or predator?

Daniel T. Haydon[1], Louise Matthews[1], Rebecca Timms[2] and Nick Colegrave[2*]

[1]*Centre for Tropical Veterinary Medicine, Easter Bush, Roslin EH25 9RG, UK*
[2]*Institute of Cell, Animal and Population Biology, University of Edinburgh, Ashworth Labs, King's Buildings, West Mains Road, Edinburgh EH9 3JT, UK*

Knowledge of the factors that limit parasite numbers offers hope of improved intervention strategies as well as exposing the selective forces that have shaped parasite life-history strategies. We develop a theoretical framework with which to consider the intra-host regulation of malaria parasite density. We analyse a general model that relates timing and magnitude of peak parasite density to initial dose under three different regulatory processes. The dynamics can be regulated either by top-down processes (upgradable immune regulation), bottom-up processes (fixed immune response and red blood cell (RBC) limitation) or a mixture of the two. We define and estimate the following key parameters: (i) the rate of RBC replenishment; (ii) the rate of destruction of uninfected RBCs; and (iii) the maximum parasite growth rate. Comparing predictions of this model with experimental results for rodent malaria in laboratory mice allowed us to reject functional forms of immune upregulation and/or effects of RBC limitation that were inconsistent with the data. Bottom-up regulation alone was insufficient to account for observed patterns without invoking either localized depletion of RBC density or merozoite interference. By contrast, an immune function upregulated in proportion to either merozoite or infected RBC density was consistent with observed dynamics. An immune response directed solely at merozoites required twice the level of activation of one directed at infected RBCs.

Keywords: malaria; *Plasmodium chabaudi*; immune regulation; parasitaemia; within-host dynamics

1. INTRODUCTION

The population dynamics of organisms has long been an obsession of ecologists, and the potential factors that can regulate population numbers are, in theory at least, well understood. Within-host dynamics of parasitic infections are increasingly viewed from the same perspective, and this approach has provided useful insight into many aspects of parasitic disease (Hellriegel 1992; Gravenor *et al.* 1995; Haydon & Woolhouse 1998; McKenzie & Bossert 1997; Molineaux & Dietz 1999; Nowak & May 2000; Simpson *et al.* 2002). Knowledge of the factors that limit parasite numbers offers hope of better-designed treatment and intervention strategies (Wilkinson *et al.* 1994; Levin & Bull 1996; Austin *et al.* 1998; Gravenor *et al.* 1998; Gravenor & Kwiatkowski 1998; McKenzie & Bossert 1998; Molineaux & Dietz 1999; Levin & Antia 2001), as well as providing information on selective forces that have moulded parasite life-history strategies.

Plasmodium chabaudi is a malaria parasite that can infect laboratory mice. It has a life cycle typical of malarial parasites—divided between a mammalian host and mosquito vector. We focus on the former. Parasites infect host red blood cells (RBCs) and undergo rounds of asexual replication. Infected RBCs rupture synchronously every 24 hours, releasing asexual progeny (merozoites) which then go on to infect new cells. This continues until the host dies, or infection is cleared. In the first 'acute' phase of infection, parasite numbers rise rapidly to a peak before crashing to very low levels. This is accompanied by host anaemia and weight loss, and possible mortality (Timms *et al.* 2001). Given the importance of the early dynamics of infection for disease severity, it is critical to understand what factors limit parasite numbers during this phase. At least three possible mechanisms could regulate parasite density: (i) a shortage of RBCs to infect (cf. bottom-up regulation); (ii) an immune response directed at merozoites and/or infected RBCs (cf. top-down regulation); or (iii) a combination of both. Discriminating between these alternatives requires a bringing together of both theory and data, and in this paper we extend this process.

We briefly review the results of an experiment that investigated the dynamics of infections of *P. chabaudi* in mice during which parasite and RBC densities were monitored daily and examined across a range of inoculation doses (Timms *et al.* 2001). We then propose a theoretical framework in which these results can be understood, estimate key parameters, and the form of the immune response, and examine the empirical results for evidence supporting these alternative hypotheses concerning regulation of infection.

* Author for correspondence (n.colegrave@ed.ac.uk).

2. EXPERIMENTAL RESULTS

Groups of mice were infected with doses of single clones ranging from 100 to one hundred million merozoites. Two parasite clones differing in virulence were used. Parasite dynamics and morbidity measures (RBC density and weight) were monitored daily (for full details of methods and results see Timms *et al.* (2001)).

The key results are that parasite dose affected both the timing and magnitude of peak parasite density irrespective of strain. Despite increasing the dose by six orders of magnitude, peak parasite density was only found to increase by 50% (figure 1*a*); and for every order of magnitude that dose was increased, this peak occurred approximately one and a half days earlier (figure 1*b*). Finally, higher parasite dose also affected morbidity—inducing greater anaemia (figure 1*c*). The overall dynamics of parasite and RBC densities for a single dose treatment are shown in figure 2*a*.

On the day of peak parasite density, RBC densities were reduced to an average of 68% (s.e. = ±3.9%) of pre-infection levels for the avirulent clone (CW), and 62% (±2.7%) for the virulent clone (BC). At this time for CW and BC, respectively, an average of 20% (±1.6%) and 39% (±2.1%) of RBCs were infected. However, for both clones, maximum anaemia typically occurred 3 days after this and, on average, RBC densities were depressed to 42% (±2.6%) of maximal levels for CW, and 19% (±1.8%) for BC.

3. THE MODEL FRAMEWORK

We use a modelling framework similar to that which has been used previously to model human malaria dynamics (Anderson *et al.* 1989; Gravenor *et al.* 1995), except that we describe the dynamics using a mixture of continuous and discrete functions (see below). We believe that this is more biologically realistic, as well as avoiding some of the potential problems with entirely continuous models (for discussion, see Gravenor & Lloyd 1998; Saul 1998; Molineaux & Dietz 1999). We consider the following set of equations to describe the dynamics of uninfected RBCs (B), infected RBCs (P) and an immune response (I). The dynamics of erythropoiesis, infected RBC destruction and immune activation are arguably continuous processes best described by differential equations:

$$\frac{dB}{dt} = s(K - B) - v(B,P,I), \tag{3.1}$$

$$\frac{dP}{dt} = -\beta PI, \tag{3.2}$$

$$\frac{dI}{dt} = P^b f(I). \tag{3.3}$$

Here, K is the 'equilibrium' density of RBCs in the absence of parasites, s is the rate at which any deficit is made up, the function $v(B,P,I)$ describes the rate at which uninfected RBCs are killed by the immune system, β is a parameter that describes the interaction of infected RBCs with the immune system, $f(I)$ is a (currently) unspecified function that describes how immune system activation depends on densities of parasites and current immune

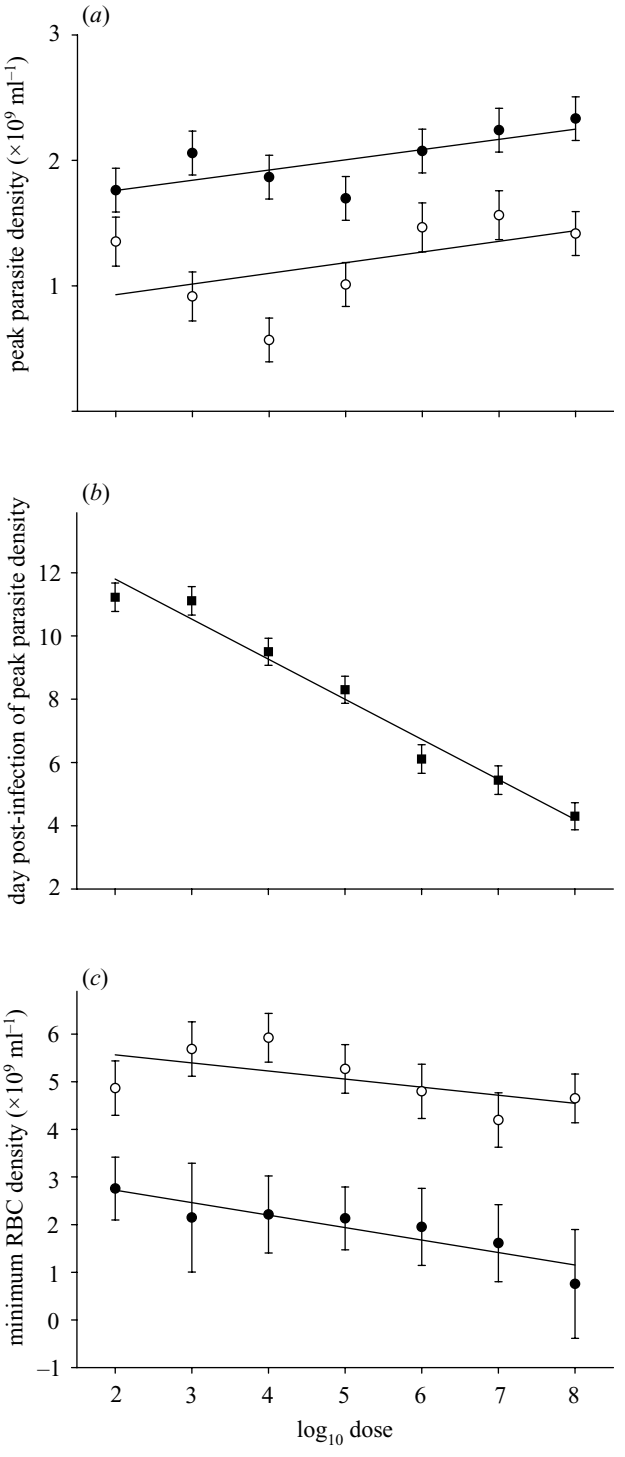

Figure 1. The effect of dose on (*a*) peak parasite density, and (*b*) the timing of peak parasite density for mice infected with the virulent (BC; filled circles) and avirulent (CW; open circles) strains. Lines are the least-squares regressions from the minimal models, which contained log dose and clone in (*a*) and log dose only in (*b*) (parasites peaked on the same day irrespective of clone, and filled squares represent both clones combined). The least-squares slopes (± s.e.) and p-values for log dose are for (*a*) 0.085 ± 0.03, $p < 0.01$ and (*b*) -0.27 ± 0.08, $p < 0.001$. (*c*) The effect of dose on $\log_{10}$ minimum RBC densities. Lines are the least-squares regressions from the minimal model, which contained log dose and clone. The least-squares slopes (± s.e.) and p-values for log dose are -0.02 ± 0.008, $p < 0.05$. (A more complete description of these results is provided by Timms *et al.* (2001).)

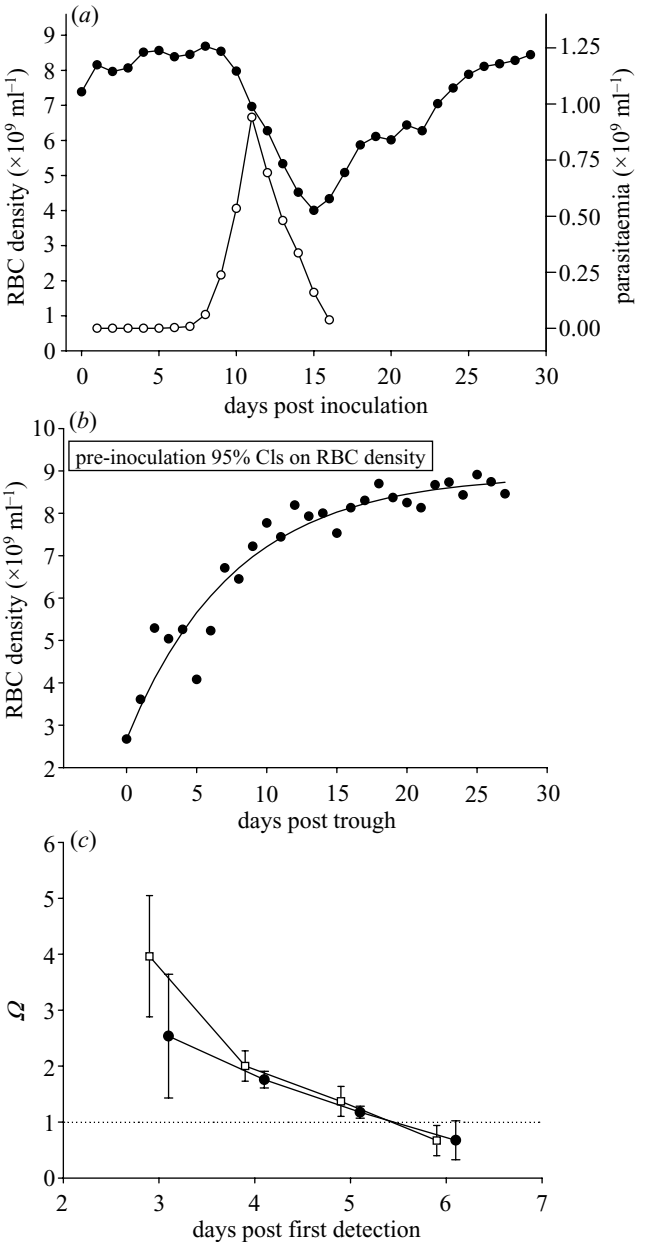

Figure 2. (*a*) The relationship between the timing of peak parasite density (open circles) and minimum RBC density (filled circles). The data shown are for the avirulent clone (CW) and the 1×10^2 dose treatment. These data are representative of the general pattern seen across other dose treatments for both clones. The lines represent the mean of five mice. (*b*) The dynamics of erythropoiesis. Data are shown for a typical mouse infected with the CW clone. Points show the actual RBC density measured and the line shows the fitted values from a model of the form $B_{\text{trough}+t} = K - \mathrm{e}^{-st}(K - B_{\text{trough}})$ (see text for details). For the data shown, the estimated value of s is 0.13. The model fits the data well ($R^2 = 0.92$), and this is typical of most mice. (*c*) The ratio of uninfected to infected RBCs eliminated by the immune system (Ω_i) as deduced using equation (4.2) for the ith day post the day of first detection of parasite density. Filled circles represent CW, open squares represent BC.

activation levels, and b a constant determining dependency of immune activation on density of infected RBCs. We disregard the negligible effect of the natural background mortality rate of infected RBCs.

Because rupture of RBCs and release of merozoites into the blood stream is a highly synchronized event in *P. chabaudi* infections, this process is best modelled discretely. If rupture occurs after fixed intervals of duration z, at times iz ($i = 1,2\ldots$), and $iz-$ indicates the time immediately prior to rupture, and $iz+$ a short time after rupture then

$$P(iz+) = Tg(B,I)P(iz-). \tag{3.4}$$

T is the maximum number of merozoites that are released into the bloodstream per infected RBC and $g(B,I)$ is a function on [0,1] that describes how this 'fecundity' falls with RBC density. We denote maximum growth, that is, the maximum number of merozoites that can go on to infect uninfected RBCs, by R(max). We do not consider gametocytogenesis, as our model investigates the early stage of a *P. chaubaudi* infection, during which rates of gametocytogenesis are minimal (Buckling *et al.* 1999).

If regulation is 'bottom-up', that is, through the availability of RBCs for infection, then analysis must focus on the parameter s and function $v(B,P,I)$ in equation (3.1), and on the form of the function $g(B,I)$ in equation (3.4). In this situation, we would assume that the immune response, while perhaps detectable, was not regulating (cf. Hellriegel 1992). If regulation is 'top-down' through immune responses, attention must be directed towards equation (3.3), parameter β in equation (3.2) and the dependency of $g(B,I)$ on I in equation (3.4). We denote values of variables at the time of peak parasite density by circumflexes (i.e. $\hat{P}$, $\hat{B}$, $\hat{I}$ and $\hat{t}$), and the value of these variables immediately following inoculation to be P_0, B_0 and I_0.

4. PARAMETER ESTIMATES

(a) *Erythropoiesis*

Erythropoiesis is thought to be upregulated during an infection and this upregulation is thought to persist after parasites have been cleared (Roth & Herman 1979; Jakeman *et al.* 1999). An increase in replacement rates of RBCs may have important consequences for the dynamics of our model. By examining the rate at which RBC density increases from its lowest point, B_{trough}, and assuming that by this time removal of infected RBCs (by rupture) and 'collateral' damage to the uninfected RBC population is small, a lower estimate on rate of replenishment can be obtained.

Assuming $v(B,P,I)$ to be small, and setting the initial condition to be equal to B_{trough}, equation (3.1) can be solved directly to give

$$B_{\text{trough}+t} = K - \mathrm{e}^{-st}(K - B_{\text{trough}}). \tag{4.1}$$

The equilibrium pre-infection RBC density (K) was estimated independently from pre-inoculation data and for all mice averaged 8.98×10^9 RBC ml^{-1}. Estimates of s were made for each clone separately using standard nonlinear regression and found to be consistent across dose treatments ($F_{1,37} = 0.09$, $p = 0.80$), but significantly different between clones ($F_{1,38} = 7.68$, $p = 0.009$): the average value of s for CW was 0.16 (s.e. = ±0.01) and for BC was 0.23 (s.e. = ±0.03). The percentage of RBCs replaced per day depends on the deficit, net daily replacement rates never exceeded 9% for CW infections and 16% for BC

infections. Figure 2*b* shows an example of the model fitted to data.

(b) *Immune destruction of uninfected RBCs*

Other models of malaria suggest that the destruction of uninfected RBCs is an important component of anaemia severity (Jakeman *et al.* 1999). We estimated the ratio of number of uninfected RBCs that are destroyed by the immune system to number of infected RBCs present, Ω_i, from

$$\Omega_i = \frac{\int_i^{i+1} v(B,I,P)\mathrm{d}t}{P_i} \approx \frac{[B_i - B_{i+1}] - P_i}{P_i}, \qquad (4.2)$$

where i refers to sampling day. The integral represents a measure of numbers of uninfected RBCs that are destroyed by the immune system between day i and $i+1$, which can be approximated by the difference between those known to be lost through the infection process and the overall change in RBC density. This difference will be positive if the reduction in RBC density is greater than that accounted for by direct destruction of parasitized cells. This method of estimating Ω_i is only applicable during the period of falling RBC density, and is unstable in the early stages of infection when counts of infected RBCs are low, and when sampling error in B_t indicates occasional small increases in RBC density about K. The expression does not account for RBCs that may have been replenished as a result of erythropoiesis, thus this estimator represents a lower bound on Ω_i. Estimated values of Ω_i for days 3–6 post day of first detection decline from just above 4 to just below 1 (figure 2*c*) and do not differ significantly between clones.

(c) R*(max)*

Let R_i be the number of merozoites that proceed to infect RBCs after the ith parasite 'generation' ($R_i \leqslant T$). We estimated the maximum number of merozoites that can go on to infect uninfected RBCs, R(max), by using the maximum value of P_{i+1}/P_i observed for each mouse. R(max) did not differ between dose treatments ($F_{1,63} = 2.71$; $p = 0.105$), but did differ significantly between clones ($F_{1,63} = 5.70$; $p = 0.020$). The average value for clone CW was 6.84 (s.e. = ±0.70) and for clone BC was 9.03 (s.e. = ±0.64). R(max) generally occurred at the first rupture event, and in the following discussion we assume that it did.

5. PREDICTIONS FROM THE MODEL

Using this theoretical framework with these parameter estimates permits a rigorous examination of the relationship between key experimental variables when regulatory processes are dominated by either 'top-down' or 'bottom-up' phenomena. Comparing these predictions with experimental results is informative about the form of immune activation functions and those governing parasite resource limitation.

6. TOP-DOWN REGULATION

Immune resources could be directed at infected RBCs, or at merozoites, or both.

(a) *Immune resources directed at infected RBCs*

In this case, regulation arises through parasite killing as indicated in equation (3.2), and the rate at which this occurs will be determined by the nature of the function and parameters in equation (3.3) which models the rate of immune activation. We consider three broad classes of functions describing immune activation: $\mathrm{d}I/\mathrm{d}t$, a constant, is a function of $I(b = 0)$, or is a function of I and $P(b > 0)$. It can be shown that if immune activation is of the form $\mathrm{d}I/\mathrm{d}t = f(I)$ then the timing of peak parasite density does not depend on dose at all, and the peak is directly proportional to initial dose (see Appendix A). These predictions are inconsistent with experimental observations and so we reject these functional forms for immune activation.

However, it can be shown that for immune activation functions proportional to $P^b \times f(I)$ (with $b > 0$) the peak parasite density is equal to $[\text{constant} + P_0^b]^{1/b}$, and the timing of the peak becomes a decreasing function of dose (see Appendix A). Using nonlinear least-squares regression of log-peak parasite density on log dose, b is estimated jointly to be 0.62 ± 0.10 (and does not differ between clones). Thus, we can deduce that the immune activation function must be, at least in the early stages of infection, dependent on parasite density.

Initially, we estimate that R(max) is 7 and 9 for the CW and BC clones, respectively. If each infected RBC actually contained T merozoites that were released into the blood stream at time t, and the level of immune activation is assumed to be constant between rupture and daily sampling time, equation (3.2) can be solved to give $P(t+\tau) = P(t)\mathrm{e}^{-\beta I(t)\tau}$ where τ is the time interval between shortly after rupture and daily sampling time. Prior to immune activation (at, say, the first rupture event) $P(z+) = TP(z-)$ and $P(z+\tau) = R_1 P(z-)$, and so $R_1 = T\mathrm{e}^{-\beta I(0)\tau}$, and $\beta I_0 \tau = -\ln(R_1/T)$. At the time of peak parasite density the observed reproductive rate (R_t) is less than or equal to 1, and therefore $\beta I(t)\tau \geqslant -\ln(1/T)$. Carter & Walliker (1975) have suggested that T is, on average, 10–12, thus with average observed R_1 values (in this case assumed to equal R(max)) of 7 and 9, we can estimate the ratio $\hat{I}/I_0$ from $-\ln(1/T)/-\ln(R_1/T)$. For the CW $\hat{I}/I_0$ is likely to be somewhere between 4 and 7 (depending on whether T is 10 or 12); and for BC $\hat{I}/I_0$ is between 9 and 22.

If there is a threshold parasite density beneath which the immune system is not activated, then parasites will be able to replicate subject only to a non-specific immune response until such time that this threshold density is surpassed. At this time, the immune system and parasite 'begin' their interaction at the initial values I_0 and $P_{\text{threshold}}$, and the effect of dose variation beneath the threshold will be irrelevant. The small but significant rise in peak parasite density observed argues against the existence of such a threshold. If there is a fixed time interval before which immune activation can begin (and during which the parasite population increased exponentially), differences in dose would be maintained and the immune system and parasite would begin their interaction at the initial values I_0 and constant $\times P_0$. Such a time-lag cannot be ruled out on the basis of these data. If infections starting with higher doses were subject to some bottom-up control then this would ameliorate the effective differences in initial condition of parasite numbers.

(**b**) ***Immune resources directed at merozoites***

In this case the growth rate is regulated directly by the immune response, hence $\beta = 0$ in equation (3.2), but $g(B,I)$ results in the immune response directly lowering its reproductive ratio. A continuous approximation to the dynamics might be $dP/dt = (c/I)P - dP$, where c/I represents a possible form for the immune-regulated growth rate and d represents removal by the fixed immune response. As before, we can consider three basic forms for the immune rate of increase: constant, dependent on the immune response, and forms of both parasite density and immune response dependent rates of increase. Using arguments essentially similar to those developed in Appendix A, it can be shown that this alternative approximation to the parasite dynamics does not qualitatively change the behaviour of the peak or its timing with respect to dose compared with when immune resources are directed at infected RBCs.

Merozoites are released synchronously at 24 hour intervals, and are widely believed to persist for only a few minutes in the bloodstream (Ramasamy *et al.* 2001). If merozoite density w time units after rupture ($w < z$), denoted by $M(w)$, is reduced by only two processes, immune killing and entry into RBCs that become infected (at rate α), then

$$\frac{dM}{dw} = -\alpha MB - \gamma MI, \tag{6.1}$$

where $M(0) = TP(iz-)$, and over this time-scale the immune system is regarded as a constant, I_c, interacting with merozoites according to a mass action term governed by coefficient γ. Dynamics of infected RBCs can be represented as

$$\frac{dP}{dw} = \alpha MB, \tag{6.2}$$

with $P(w = 0) = 0$, and uninfected RBCs by

$$\frac{dB}{dw} = -\alpha MB. \tag{6.3}$$

This assumes that there is no opportunity for multiple infection of RBCs, but models that do allow multiple infection show that it has negligible effects on dynamics (Hetzel & Anderson 1996). If immune resources are directed solely at merozoites, and infected RBCs are not removed prior to releasing merozoites, the maximum density of infected RBCs over the course of this round of replication, denoted $P(\max)$, will have occurred just prior to the ith + 1 rupture event. The observed growth rate of infected RBCs as a result of the ith rupture event is then

$$R(i) = \frac{P(\max)}{P(iz-)}. \tag{6.4}$$

In Appendix B we show equations (6.1)–(6.3) can be solved to give an expression for this maximum:

$$P(\max) \approx \frac{TP(iz-)B_0}{B_0 + \gamma I_c/\alpha} \tag{6.5}$$

and thus $R(i)$ can be estimated as

$$R(i) \approx \frac{TB(iz-)}{B(iz-) + \gamma I_c/\alpha}. \tag{6.6}$$

With $R(i)$ varying between less than 1 and 7 (CW) and less than 1 and 9 (BC), and if RBCs are not limiting, decline in growth rate must be brought about by increases in I_c with each sequential rupture (i.e. γI in equation (6.1)). This indicates that $\hat{I}_c/I_c(0) = \hat{B}R_1(T-1)/B_0(T-R_1)$ and that with R_1 values of 7 and 9, and T of 10–12, $\hat{I}_c/I_c(0)$ would be in the range of 10–15 for CW, and 20–50 for BC.

7. BOTTOM-UP REGULATION

In this case immune killing is assumed to be minimal, and infection is governed by $g(B,I)$ in equation (3.4) which, as suggested by equation (6.6), might take the form $g(B,I) = (c_1B)/(c_2I_0 + c_3B)$ where c_is are positive constants. However, an obvious problem immediately becomes apparent. Since $(\partial^2 g/\partial B^2) < 0$ for all RBC densities, g cannot be a concave function of B, furthermore, this curve might reasonably be expected to pass through the origin (figure 3*a*). The experimental evidence suggests that a 40–50% decrease in RBC density results in a *ca.* 80% decrease in R (figure 3*b*,*c*) but such a steep decline cannot be brought about by a function of the form $g(B,I) = (c_1B)/(c_2I_0 + c_3B)$.

What, apart from an increase in immune activity, could account for the insufficiency of this function? It is possible that the function is structurally appropriate but that the actual density of RBCs available to merozoites differs from our empirical estimates of RBC density. Perhaps, as a result of sequestration of infected RBCs in smaller blood vessels prior to rupture, and a consequent reduction in blood flow ('sludging'), local uninfected RBC availability is less than that estimated to be circulating more generally. However, to bring the growth rate down to 1, the local density would have to be, at most, one-fifth of the observed RBC density at the time of peak parasite density.

Figure 4 shows how the full model (equations (3.1)–(3.4)), in which both top-down and bottom-up processes operate simultaneously, could be fitted to these data. The close fit between the full model and the observed data is not surprising given the number of parameters that the model contains. However, the main aim of this paper is not to provide a detailed description of the dynamics of this particular experiment, rather it is to elucidate which combinations of mechanisms could potentially explain the dynamics.

8. DISCUSSION

We have assembled a theoretical framework with which to examine mechanisms of regulation of the acute phase of malaria parasite density. This framework is very general and, initially, only sets out to define the 'envelope' within which dynamics of regulation must reside. We use it here for three purposes: (i) to identify and define key parameters that govern dynamics of variables involved in regulation; (ii) to suggest ways in which some of these parameters might be estimated from data; and (iii) to predict the 'signatures' of parasite density dynamics that result from different assumptions regarding the functional form of key regulatory processes.

Specifically, we define and quantify the dynamics of RBC replacement, immune destruction of uninfected

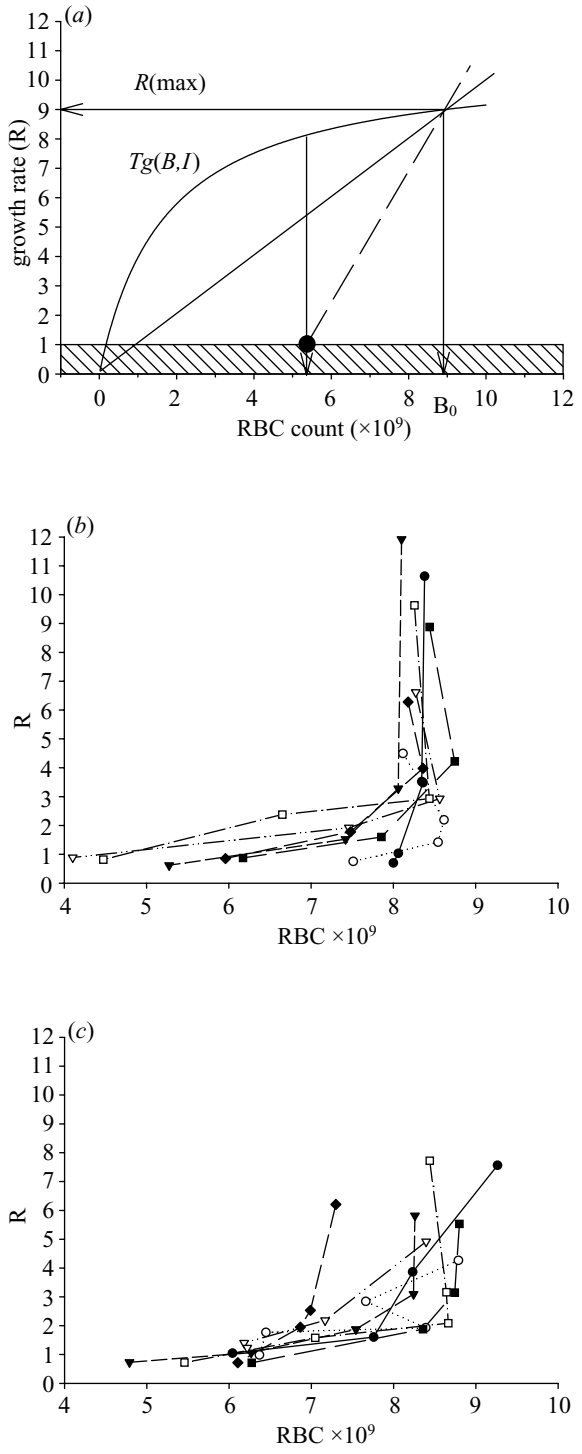

Figure 3. The dynamics of bottom-up infection. (*a*) The function $Tg(B,I)$ is anticipated to define a curve that is either convex (upper curve) or appears almost linear (straight line). However, neither shape can explain the required change in the growth rate from R(max) (of 7 or 9) to less than 1, which occurs with only a 40% change in RBC density (down to $5–6 \times 10^9$ cells ml^{-1}). (*b*) A plot showing the corresponding empirical overlay to (*a*) with observed growth rates and associated RBC densities of the virulent clone (BC) plotted by dose and joined by a line reflecting the temporal order in which they were observed (one measurement per day). Filled circles, 10^2; open circles, 10^3; filled inverted triangles, 10^4; open inverted triangles, 10^5; filled squares, 10^6; open squares, 10^7; filled diamonds, 10^8. (*c*) The same plot for the avirulent clone (CW). Note the highly concave form of the curves in (*b*) and (*c*).

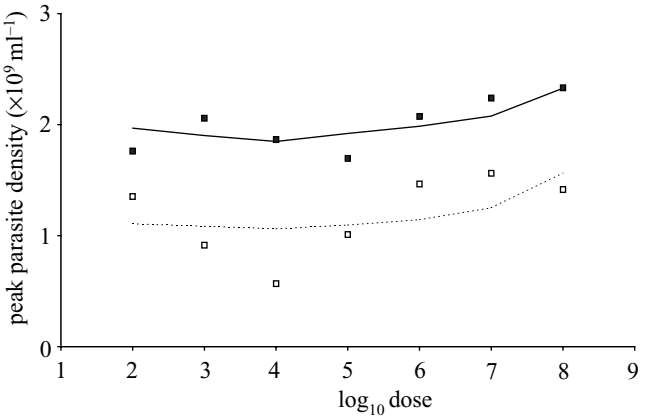

Figure 4. The full model (equations (3.1)–(3.4)) fitted to peak parasite density for the BC clone (black squares) and the CW clone (open squares). The model assumes that the immune response is directed at the merozoites. Accordingly, equation (6.6) (see text for details) is used to update the total RBCs and infected RBCs at each parasite generation. The immune response, I_c, increases at each parasite generation according to a discretized version of $dI_c/dt = kP^b$. A scaling factor is introduced to allow for the fact that not all of the initial dose may survive to infect a RBC. For consistency of model outputs with prior estimates of T we set this scale factor equal to 0.5 for both clones. The value of b (±s.e.) is estimated jointly for both clones to be 0.62 ± 0.10. The parameters k and T are fitted (by minimizing the sum of squares) independently for each clone. The estimated values of k and T are 5.3 and 14.4 for clone BC and 6.0 and 9.5 for clone CW. R^2 values are 0.56 for model fit to BC clone (solid line) and 0.28 for the model fit to the CW clone (dotted line).

RBCs, and maximum growth rates of merozoites. We highlight the potential value of determining the number of merozoites that infected RBCs release into the bloodstream in revealing the extent to which the immune system may be upregulated. We proceed by providing direct experimental evidence that available data strongly support the notion that activation of immune responses must be dependent on parasite densities, and that the data are not readily explained solely through bottom-up regulation, as a consequence of restricted availability of RBCs.

The experimental data on erythropoiesis suggest that RBCs are resupplied at a rate proportional to the RBC deficit. However, the rate constant differs significantly between clones. Anaemia was significantly greater for virulent infections (19% of uninfected levels) compared with avirulent infections (42% of uninfected levels), consistent with the idea that as anaemia becomes more acute, qualitatively different means of RBC resupply are stimulated.

Estimates of the ratio of immune destruction of uninfected to infected RBCs are complicated in the early stages of infection by the slight and fluctuating estimates of anaemia, and in the late stages of infection by the upregulation of erythropoiesis. Nonetheless, we estimate this ratio to be between 1 and 4, irrespective of clone. However, our method of estimation is likely to result in these being only lower estimates, and other methods have found higher ratios. Using a model that included erythropoiesis, Jakeman *et al.* (1999) estimated that, in malaria caused by *Plasmodium falciparum*, for every infected RBC, around

8.5 uninfected RBCs were removed by the immune system. However, it is not clear whether this difference is due to differing model assumptions, or real biological differences between murine and human malarias. Similarly, the marked decline in our estimates of this ratio could arise because erythropoiesis masks the real level of destruction of uninfected RBCs, or because the immune response changes over the early stages of infection (for example, the proposed switch from a predominantly type 1 T-cell-dependent response to a type 2 response suggested to occur during an infection; Taylor-Robinson & Phillips 1994).

The maximum growth rates are found to differ between clones. This could arise for at least three different reasons. First, the virulent clone may possess some feature that renders merozoites, or the cells they infect, less apparent to immune agents. Second, merozoites of the virulent clone may be more efficient at infecting RBCs, reducing the impact of immune responses directed at merozoites, and/or the reduction in RBC density. Third, RBCs infected with the virulent clone may release a larger number of merozoites into the bloodstream. Given that these maximum growth rates are observed in the initial stages of infection when anaemia and immune regulation are less influential, we consider the third explanation to be the most likely (see Simpson *et al.* 2002). If regulation was entirely top-down, then our model predicts that the virulent clone should release *ca*. 20% more merozoites into the bloodstream, relative to the avirulent clone, if differences in peak density (figure 1*a*) are to be explained. This proposal is testable by direct observation of infected RBCs just prior to rupture.

Unfortunately this analysis does not permit an inference to be made about which parasite life-history stage immune resources are directed at. The model predicts that if immune resources are directed at infected RBCs, the level of immune stimulation over pre-infected levels need be only half that compared with that if immune resources are directed at merozoites. That an immune response directed against infected RBCs is more effective than one against merozoites is a common conclusion of models of malaria infections, although the reasons differ between models (Anderson *et al.* 1989; Hetzel & Anderson 1996). In our model it occurs because every infected RBC taken out by the immune system is equivalent to the destruction of at least 10–12 merozoites (and possibly more depending on the value of T). There is evidence for protective immune responses directed against both merozoites (Conway *et al.* 2000) and infected RBCs (Bull *et al.* 1998) in malaria infections. However, as far as we are aware there is no current estimate of the relative importance of each in removing parasites. Measuring T is important since it will permit a direct estimate of the 'functional extent' of immune upregulation, a quantity that is rarely estimable in terms of the direct effect of the immune system on a pathogen.

Theoretical models of immune dynamics are commonplace in the literature, often resting on largely unsubstantiated assumptions regarding the form of immune activation and its dependence on pathogen density. We argue that the overall upregulation of immune resources must be dependent on pathogen density. No other simple functional form accounts for the experimental results described. Upregulation appears not to be directly proportional to parasite density, but to a quantity approximately corresponding to the square root of parasite density ($b \sim 0.6$ for both clones). We tentatively interpret this as suggestive of some finite immune capacity to process antigen, perhaps immune receptor saturation.

Our analysis indicates that the experimental data are essentially inconsistent with a solely bottom-up explanation for regulation of parasite density. This contrasts with the conclusions of Hetzel & Anderson (1996), that immune regulation is not necessary to explain the magnitude of the initial peak in parasite numbers in *P. berghei* infections of mice, but is in agreement with that of the examination of human malaria dynamics by Gravenor *et al.* (1995). The difficulty is in finding plausible explanations for the required shape of the function governing the relationship between RBC density and parasite growth rates. Parsimonious hypotheses suggest that this function is (at best) likely to appear linear, if not convex (*sensu* figure 3*a*), when the data require that it be quite dramatically concave (figure 3*b*,*c*). Only with this concavity is it possible to explain an 80% decrease in growth rate (7 or 9 down to less than 1) with only a 40% reduction in RBC density. However, there is some empirical evidence to suggest that bottom-up regulation may play some part in regulation. Individuals that had their anaemia alleviated by transfusion maintained higher levels of parasites than individuals that were given no extra blood (ducks, Rigdon & Varnadoe 1945; mice, Yap & Stevenson 1994). Bottom-up explanations for regulation become more tenable if merozoites interfere with each other's access to the RBC population as parasite density increases. A possible mechanism for such interference is if characteristics of blood flow change substantially over the course of parasite density. For example, if infected RBCs sequester in narrow capillaries prior to rupture (Newbold *et al.* 1999), this would have the effect of restricting the flow of uninfected RBCs through these capillaries at exactly the time that the parasite might most benefit from improved access to the uninfected RBC population. Similarly, if parasites only use a subset of the total population of RBCs, the drop in the total population of RBCs would underestimate the drop in the usable population. Either of these mechanisms could provide the required nonlinearity between overall RBC density and growth rate obvious from figure 3*b*,*c*. However, such an effect would have to effectively reduce RBC density to *ca*. 20% of its actual value at the time of peak parasite density. Clones of parasites that vary in their ability to sequester do not differ in their growth rate (Gilks *et al.* 1990) and this suggests that local depletion due to sequestration is unlikely to play an important part, whilst the fact that *P. chaubaudi* is thought to use RBCs non-preferentially with respect to age (Jarra & Brown 1989) argues against the latter explanation. The evidence presented does not rule out a role for bottom-up regulation, but does strongly suggest that regulation cannot be solely bottom-up.

Malaria infections are notoriously complicated, resulting from a complex interaction of many variables, heterogeneously dispersed in space (throughout the body) and time (throughout the course of infection). As with our understanding of many other dynamic biological systems, further progress will be greatly facilitated by a more inti-

mate linking of theory and data. Such interplay will aid theoretical progress—in terms of shrinking the volume of parameter space within which infection dynamics are modelled, thereby rendering models more insightful. But also, in turn, such models will indicate areas in which only careful experimentation can tease apart competing functional forms governing the interaction of relevant variables, and which parameters are most worthy of experimental evaluation. This paper is intended as an example of the value of such a combined approach.

The authors thank Margaret Mackinnon, Mike Gravenor and particularly Louise Taylor for very helpful insights during the course of this analysis and two anonymous reviewers for helpful comments. D.T.H. and L.M. are grateful to the Wellcome Trust for financial support.

APPENDIX A

(a) *Peak parasite density and dose*

Assume a functionally equivalent union of equations (3.2) and (3.4), so that the parasite population, which is assumed to have a per capita growth rate of r, grows continuously according to the equation

$$\frac{dP}{dt} = rP - \beta PI$$

and that the initial value of P is P_0, and peaks at density $\hat{P}$, when $I = \hat{I} = r/\beta$.

(i) Consider that immune resources are activated at a constant rate c. Thus $dI/dt = c$, and starts from a baseline activation level I_0. So $I(t) = I_0 + ct$, the time of the peak is given by $\hat{t} = (r - \beta I_0)/(\beta c)$ and $\hat{P} = P_0 \exp((\beta I_0 - r)^2/2\beta c)$.

(ii) Consider that immune resources are activated at an exponential rate c. Thus, $dI/dt = cI$ and $I(t) = I_0 \exp(ct)$. The time of the peak is given by $\hat{t} = (1/c)\ln(r/\beta I_0)$ and $\hat{P} = P_0 \exp(r\hat{t} + (\beta I_0/c)(1 - e^c))$.

In general, if $dI/dt = f(I)$ then $I(t)$ does not depend on dose, and since peak parasitaemia occurs at $\hat{t}$ such that $I(\hat{t}) = r/\beta$, the timing of the peak is independent of dose.

(i) Consider immune activation functions of the form $dI/dt = P^b f(I)$ and a parasite growth rate determined by the general form $dP/dt = Pg(I)$. Parasite density peaks at $\hat{P}$ when $I = \hat{I}$ which satisfies $g(\hat{I}) = 0$.

Substituting $U = P^b$, gives $(1/bU)(dU/dt) = (1/P)(dP/dt)$ which enables rewriting the equations in the form $(1/b)(dU/dt) = Ug(I)$ and $dI/dt = Uf(I)$. Now $(1/b)(dU/dI) = g(I)/f(I)$ which gives $(1/b)U = (1/b)U_0 + h(I) - h(I_0)$, or equivalently

$$\frac{1}{b}P^b = \frac{1}{b}P_0^b + h(I) - h(I_0),$$

where P_0 and I_0 are the initial values of P and I and $h(I) = \int (g(I)/f(I))dI$. Thus, peak parasite density $\hat{P}$ and dose P_0 are related by

$$\frac{1}{b}\hat{P}^b = \frac{1}{b}P_0^b + h(\hat{I}) - h(I_0).$$

Using the above expression for P^b we can rewrite the equation for the dynamics of the immune system as

$$\frac{dI}{dt} = f(I)(P_0^b + bh(I) - bh(I_0)).$$

Differentiating with respect to P_0 we obtain

$$\frac{\partial(dI/dt)}{\partial P_0} = bP_0^{b-1} f(I) > 0.$$

Thus, the rate of increase of the immune response I increases with increasing P_0. Since the peak parasitaemia occurs when I reaches a fixed level, the timing of the peak must decrease with increasing dose.

(b) *Examples*

If the dependence of the immune activation function on I is constant, $f(I) = c$, and $g(I) = r - \beta I$ we obtain $\hat{I} = r/\beta$ and $h(I) = (1/c)(rI - (\beta/2)I^2)$. Hence,

$$\frac{1}{b}\hat{P}^b = \frac{1}{b}P_0^b + \frac{\beta}{2c}\left(I_0 - \frac{r}{\beta}\right)^2.$$

If the dependence of the immune activation function on I is proportional to I, $f(I) = cI$, and $g(I) = r - \beta I$ we obtain $h(I) = (1/c)(r\ln I - \beta I)$ and $\hat{I} = r/\beta$. Hence,

$$\frac{1}{b}\hat{P}^b = \frac{1}{b}P_0^b + \frac{\beta}{c}\left(\frac{r}{\beta}\ln\left(\frac{r}{\beta I_0}\right) + I_0 - \frac{r}{\beta}\right).$$

(c) *Timing of peak with respect to dose*

If $dI/dt = cP^b$ and $dP/dt = rP - \beta PI$ then the coupled set of equations for I and P can be solved directly to give an expression for the time of peak, $\hat{t}$. Again, making the substitution $U = P^b$ we obtain the pair of equations

$$\frac{1}{b} \times \frac{dU}{dt} = U(r - \gamma I) \text{ and } \frac{dI}{dt} = cU,$$

which yield

$$\frac{1}{b} \times \frac{dU}{dI} = \frac{r - \beta I}{c}$$

and hence, $(1/b)U = (1/c)(rI - (\beta I^2/2)) + d \equiv -(\beta/2c) \times (I^2 - 2(r/\beta)I + d')$ where d,d' are arbirtrary constants. We may rewrite this expression in the form

$$\frac{1}{b}U = -\frac{\gamma}{2c}\left[(I - a)\left(I - \left(\frac{2r}{\gamma} - a\right)\right)\right],$$

where $a = (r/\gamma)(1 - \sqrt{q})$ and q is given by $q = 1 - (\beta/r)^2 d'$. Hence,

$$\frac{1}{b}\frac{dI}{dt} = -\frac{\gamma}{2}\left[(I - a)\left(I - \left(\frac{2r}{\gamma} - a\right)\right)\right],$$

which can be integrated to give

$$\frac{1}{(r - \gamma a)}\ln\left|\frac{I - a}{I - (2r/\gamma - a)}\right| = bt + k$$

where k is an arbitrary constant.

At $t = 0$, $U = U_0 = P_0^b$ and $I = I_0$. Thus,

$$d' = 2\frac{r}{\beta}I_0 - I_0^2 - \frac{2c}{\beta} \times \frac{1}{b}P_0^b \text{ and } k = \frac{1}{(r - \beta a)}\ln\left|\frac{I_0 - a}{I_0 - (2r/\beta - a)}\right|.$$

At peak parasite density, $I = r/\beta$, and thus the time of the peak, $\hat{t}$, is given by

$$\hat{t} = \frac{-k}{b}.$$

APPENDIX B

Assume the dynamics of merozoites M, infected RBCs P and uninfected RBCs B, at time w after rupture can be represented by

$$\frac{dM}{dt} = -\alpha MB - \gamma MI_c, \frac{dB}{dt} = -\alpha MB \text{ and } \frac{dP}{dt} = \alpha MB,$$

where I_c is assumed to be a constant immune response. Dividing the equations for M and B gives

$$\frac{dM}{dB} = 1 + \frac{\gamma I_c}{\alpha} \times \frac{1}{B},$$

which on integration yields

$$M = B + \frac{\gamma I_c}{\alpha} \ln B + M_0 - B_0 - \frac{\gamma I_c}{\alpha} \ln B_0,$$

where M_0 and B_0 are the densities of merozoites and uninfected RBCs at $w = 0$. We wish to determine the density of uninfected RBCs, B, when all the merozoites have either occupied RBCs or been removed by the immune system. Setting $M = 0$ we obtain

$$M_0 = B_0 - B - \frac{\gamma I_c}{\alpha} \ln \frac{B}{B_0}.$$

Setting $B_0 - B = \Delta B$ gives

$$M_0 = \Delta B - \frac{\gamma I_c}{\alpha} \ln\left(1 - \frac{\Delta B}{B_0}\right).$$

Thus, for ΔB much less than B_0, we obtain

$$M_0 = \Delta B - \frac{\gamma I_c}{\alpha}\left(-\frac{\Delta B}{B_0}\right) + O\left(\frac{\Delta B}{B_0}\right)^2,$$

that is, $M_0 \approx \Delta B(1 + (\lambda I_c/\alpha B_0))$.

Since the maximum number of infected RBCs, $P(\max)$ is equal to the reduction in uninfected RBCs, ΔB, and $M_0 = TP(iz-)$, we obtain

$$P(\max) \approx \frac{TP(iz-)B_0}{B_0 + \gamma I_c/\alpha}.$$

REFERENCES

Anderson, R. M., May, R. M. & Gupta, S. 1989 Non-linear phenomena in host–parasite interactions. *Parasitology* **99**, S59–S79.

Austin, D. J., White, N. J. & Anderson, R. M. 1998 The dynamics of drug action on the within-host population growth of infectious agents: melding pharmacokinetics with pathogen population dynamics. *J. Theor. Biol.* **194**, 313–339.

Buckling, A., Crooks, L. & Read, A. 1999 *Plasmodium chabaudi*: the effect of anti-malarial drugs on gametocytogenesis. *Exp. Parasitol.* **93**, 45–54.

Bull, P. C., Lowe, B. S., Kortok, M., Molyneux, C. S., Newbold, C. I. & Marsh, K. 1998 Parasite antigens on the infected red cell surface are targets for naturally acquired immunity to malaria. *Nature Med.* **4**, 358–360.

Carter, R. & Walliker, D. 1975 New observations of the malaria parasites of the Central African Republic, *Plasmodium vinckei petteri* subsp. nov and *P. chabaudi* Landau (1965). *Ann. Trop. Med. Parasitol.* **69**, 187–196.

Conway, D. J. (and 11 others) 2000 A principal target of human immunity to malaria identified by molecular population genetic and immunological analyses. *Nat. Med.* **6**, 689–692.

Gilks, C. F., Walliker, D. & Newbold, C. I. 1990 Relationships between sequestration, antigenic variation and chronic parasitism in *Plasmodium chabaudi chabaudi*—a rodent malaria model. *Parasitol. Immunol.* **12**, 45–64.

Gravenor, M. B. & Kwiatkowski, D. 1998 An analysis of the temperature effects of fever on the intra-host population dynamics of *Plasmodium falciparum*. *Parasitology* **117**, 97–105.

Gravenor, M. B. & Lloyd, A. L. 1998 Reply to: models for the in-host dynamics of malaria revisited: errors in some basic models lead to a large over estimate of growth rate. *Parasitology* **117**, 409–410.

Gravenor, M. B., Mclean, A. R. & Kwiatkowski, D. 1995 The regulation of malaria parasitemia—parameter estimates for a population-model. *Parasitology* **110**, 115–122.

Gravenor, M. B., Van Hensbroek, M. B. & Kwiatkowski, D. 1998 Estimating sequestered parasite population dynamics in cerebral malaria. *Proc. Natl Acad. Sci. USA* **95**, 7620–7624.

Haydon, D. T. & Woolhouse, M. E. J. 1998 Immune avoidance strategies in RNA viruses: fitness continuums arising from trade-offs between immunogenicity and antigenic variability. *J. Theor. Biol.* **193**, 603–612.

Hellriegel, B. 1992 Modeling the immune response to malaria with ecological concepts—short-term behavior against long-term equilibria. *Proc. R. Soc. Lond.* B **250**, 249–256.

Hetzel, C. & Anderson, R. M. 1996 The within-host cellular dynamics of bloodstage malaria—theoretical and experimental studies. *Parasitology* **113**, 25–38.

Jakeman, G. N., Saul, A., Hogarth, W. L. & Collins, W. E. 1999 Anaemia of acute malaria infections in non-immune patients results from destruction of uninfected erythrocytes. *Parasitology* **119**, 127–133.

Jarra, W. & Brown, K. N. 1989 Invasion of mature and immature erythrocytes of CBA/Ca mice by a cloned line of *Plasmodium chabaudi chabaudi*. *Parasitology* **99**, 157–163.

Levin, B. R. & Antia, R. 2001 Why we don't get sick: the within-host population dynamics of bacterial infections. *Science* **292**, 1112–1115.

Levin, B. R. & Bull, J. J. 1996 Phage therapy revisited: the population biology of a bacterial infection and its treatment with bacteriophage and antibiotics. *Am. Nat.* **147**, 881–898.

McKenzie, F. E. & Bossert, R. H. 1997 The dynamics of *Plasmodium falciparum* blood-stage dynamics. *J. Theor. Biol.* **188**, 127–140.

McKenzie, F. E. & Bossert, W. H. 1998 A target for intervention in *Plasmodium falciparum* infections. *Am. J. Trop. Med. Hyg.* **58**, 763–767.

Molineaux, L. & Dietz, K. 1999 Review of intrahost models of malaria. *Parasitologia* **41**, 221–231.

Newbold, C., Craig, A., Kyes, S., Rowe, A., Fernandez-Reyes, D. & Fagan, T. 1999 Cytoadherence, pathogenesis and the infected red cell surface in *Plasmodium falciparum*. *Int. J. Parasitol.* **29**, 927–937.

Nowak, M. A. & May, R. M. 2000 *Virus dynamics*. Oxford University Press.

Ramasamy, R., Ramasamy, M. & Yasawardena, S. 2001 Antibodies and *Plasmodium falciparum* merozoites. *Trends Parasitol.* **17**, 194–197.

Rigdon, R. H. & Varnadoe, N. B. 1945 Transfusions of red

cells in malaria: an experimental study in ducks. *Am. J. Trop. Med.* **25**, 409–415.

Roth, R. L. & Herman, R. 1979 *Plasmodium berghei*: correlation of *in vitro* erythrophagocytosis with the dynamics of early onset anaemia and reticulocytosis. *Exp. Parasitol.* **47**, 169–179.

Saul, A. 1998 Models for the in-host dynamics of malaria revisited: errors in some basic models lead to a large over estimate of growth rate. *Parasitology* **117**, 405–407.

Simpson, J. A., Aarons, L., Collins, W. E., Jeffery, G. M. & White, N. J. 2002 Population dynamics of untreated *Plasmodium falciparum* malaria within the adult human host during the expansion phase of the infection. *Parasitology* **124**, 247–263.

Taylor-Robinson, A. W. & Phillips, R. S. 1994 B-cells are required for the switch from Th1- to Th2-regulated immune responses to *Plasmodium chabaudi chabaudi* infection. *Infect. Immun.* **62**, 2490–2498.

Timms, R., Colegrave, N., Chan, B. H. K. & Read, A. F. R. 2001 The effect of parasite dose on disease severity in the rodent malaria *Plasmodium chabaudi*. *Parasitology* **123**, 1–11.

Wilkinson, R. J., Brown, J. L., Pasvol, G., Chiodini, P. L. & Davidson, R. N. 1994 Severe *falciparum* malaria: predicting the effect of exchange transfusion. *Q. J. Med.* **87**, 553–557.

Yap, G. S. & Stevenson, M. M. 1994 Blood transfusion alters the course and outcome of *Plasmodium chabaudi* AS infection in mice. *Infect. Immun.* **62**, 3761–3765.

As this paper exceeds the maximum length normally permitted, the authors have agreed to contribute to production costs.